

# Jammed lattice sphere packings

Yoav Kallus\*

*Princeton Center for Theoretical Science, Princeton University, Princeton, New Jersey 08544*

Étienne Marcotte

*Department of Physics, Princeton University, Princeton, New Jersey 08544*

Salvatore Torquato

*Department of Physics, Princeton University, Princeton, New Jersey 08544*

*Department of Chemistry, Princeton University, Princeton, New Jersey 08544*

*Program in Applied and Computational Mathematics,*

*Princeton University, Princeton, New Jersey 08544 and*

*Princeton Institute of the Science and Technology of Materials,*

*Princeton University, Princeton, New Jersey 08544*

(Dated: September 16, 2021)

We generate and study an ensemble of isostatic jammed hard-sphere lattices. These lattices are obtained by compression of a periodic system with an adaptive unit cell containing a single sphere until the point of mechanical stability. We present detailed numerical data about the densities, pair correlations, force distributions, and structure factors of such lattices. We show that this model retains many of the crucial structural features of the classical hard-sphere model and propose it as a model for the jamming and glass transitions that enables exploration of much higher dimensions than are usually accessible.

PACS numbers: 61.50.Ah, 05.20.Jj, 61.43.-j

## I. INTRODUCTION

There are many reasons for studying jammed sphere packings in Euclidean spaces of high dimension. For one, sphere packing in high dimensions has direct applications for constructing codes in communication and information theory [1]. A classical result of Minkowski provides a non-constructive lower bound on the optimal packing density in  $d$ -dimensional Euclidean space,  $\varphi > 2^{-d+1}$ , and this lower bound is achieved by a Bravais lattice packing [2]. However, no general construction is known that achieves this bound in arbitrary dimension, either by a lattice or a nonlattice packing [1]. The current asymptotically-best bound is given by Ball,  $\varphi > 2d2^{-d}$  [3]. Random processes have been described that seem to satisfy the asymptotic behavior described by Minkowski's bound, and in some cases to give polynomial corrections to it,  $\varphi \sim d^\nu 2^{-d}$ . Such processes include random sequential addition (RSA) [4], ghost RSA [5], and compression of a hard-sphere fluid [6, 7]. These processes all result in non-lattice packings of immense complexity. Here we describe a random process that yields Bravais lattice packings and that seems to give a larger polynomial correction to Minkowski's bound than previously described processes,  $\varphi \sim d^\nu 2^{-d}$  with  $\nu \approx 3$ .

Perhaps more importantly, investigating jammed sphere packings in high dimensions has the clear potential of advancing our fundamental understanding of

granular matter and structural glasses in three dimensions: by going to higher dimensions, not only do we circumvent some of the technical difficulties encountered in low dimensions – e.g., the presence of rattlers [6] and the tendency to form crystallites [8] – but we also stand to resolve many ongoing theoretical disputes if we can determine how crucial quantities like the jamming density scale as a function of dimension [7, 9–12]. However, the increased difficulty of simulating systems in higher dimensions has been a major roadblock in taking full advantage of their potential to guide the field forward. Pioneering work has studied jammed sphere packings in up to 6 dimensions [6, 13], and recent heroic efforts have obtained data for densities in up to 13 dimensions [14]. Still, detailed structural data is only available in up to 10 dimensions [14]. We find that Bravais lattices are simple enough to study in these, and much higher, dimensions, and yet complex enough that in high enough dimensions they exhibit all the phenomena of interest in the study of disordered packing.

Jammed configurations of (frictionless) hard spheres are those in which any motion of the spheres necessary requires an increase in the volume of the system. These configurations are characterized by mechanical stability: as long as the volume of the system is held fixed, the system can resist any set of forces applied to its constituents. Here we propose to study the jamming behavior of a related system, the hard-sphere lattice model. A  $d$ -dimensional lattice sphere packing is a periodic arrangement of non-overlapping spheres in Euclidean space  $\mathbb{R}^d$  with a single sphere per unit cell, that is, a Bravais lattice (we will henceforth use the word *lattice* to refer

---

\*Electronic address: ykallus@princeton.edu

exclusively to Bravais lattices). In the hard-sphere lattice model, the lattice in question is the dynamic variable, and the sphere centers occupy all lattice sites. One should not confuse this kind of lattice model with the more common meaning of *lattice model*, where the underlying lattice is fixed and particles move from site to site. We show that the hard-sphere lattice model allows us to study many of the same phenomena that are of interest in the classical hard-sphere model, which includes the equilibrium phase diagram, as well as jammed states, disordered or not. We will henceforth use the modifiers *lattice* and *classical* to differentiate between phenomena as they occur in the lattice model and in the classical hard-sphere model. With the lattice hard-sphere model, we can study these phenomena in much higher spatial dimensions than accessible in the classical model: we obtain and analyze detailed structural data in up to 24 dimensions. Especially in high dimensions and in the limit  $d \rightarrow \infty$  there are reasons to expect some similarities between the lattice and classical hard-sphere models [15, 16].

The classical hard-sphere model has been invaluable in the study of materials: it is a useful model for the liquid state [17], the fluid-solid transition [18], the glass transition [19], granular flow [20], exotic melting behavior in two dimensions [21], and countless other phenomena. Much like the classical hard-sphere model has been incredibly useful in the study of many phenomena, the recent wave of work on hard-sphere lattices demonstrates that this versatility by and large carries over to the lattice setting as well: Parisi established a liquid state theory of lattice sphere packings [15], we have previously focused on the ground state [22, 23], and here we focus on jamming.

Our results indicate that the typical density of jammed hard-sphere lattices is likely to be much higher than the density of a classical jammed hard-sphere configuration in the same dimension. The mean packing fraction of a jammed hard-sphere lattice appears, based on our analysis (see Section IV.A), to scale asymptotically as  $\varphi \sim d^\nu 2^{-d}$ , with  $\nu = 3.01 \pm 0.01$ . In contrast, estimates and predictions for classical jammed hard spheres give asymptotic scaling with an exponent  $1 \leq \nu \leq 2$  [7, 24]. The fact that jammed hard-sphere lattices seem to be much denser than classical jammed configurations might come as a surprise, because in the case of the optimal packing, the densest configurations are expected to be much more dense than the densest (Bravais) lattice configurations in most high-enough dimensions [5]. However, the fact that jammed lattices must have at least  $d(d+1)$  contacts around each sphere, compared to an average of  $2d$  contacts in a classical jammed configuration (see Section II), suggests that we might also expect higher densities.

We report here pair correlation functions and contact force distributions similar to the ones observed in the classical setting. In particular, we observe power law behaviors for the distribution of weak contact forces and

for the near-contact pair correlation. The power law exponents do not depend on dimension, but they are different than those observed in the classical model [14]. In Section II, we will give some background and formulate the lattice sphere packing problem as an optimization problem. This formulation gives rise to the description of contact forces in a jammed packing as Lagrange multipliers. In Section III, we will describe the procedure by which we construct ensembles of isostatic extreme lattices in dimensions 15 to 24. In Section IV, we describe our observations of that ensemble, summarized above. We end with some closing remarks in Section V.

## II. THEORY

The study of lattices as a special case of sphere packing in arbitrary dimensions has a long and celebrated history [1, 25]. In the physical setting, lattices have been considered as ordered phases of hard-sphere systems, but the behavior of a system restricted to take only lattice configurations has only recently begun to draw serious study [15]. Parisi considered the problem of calculating the entropy of such a system as a function of unit cell volume. He uses results of Rogers as a starting point to derive the basic tools and techniques needed to establish a formal statistical mechanics theory of lattice sphere packings [15]. The second- and third-named authors studied the behavior of the system under rapid compression using the Torquato-Jiao algorithm [13, 22]. The first-named author performed quasistatic compression simulations using a Monte Carlo method, which showed that the system experiences a fluid-solid crystallization transition in moderately high dimensions [23].

The use of the terms *fluid* and *crystallization* might be confusing or seem inappropriate when all configurations considered are *a priori* lattices and therefore ostensibly crystalline. However, in light of the fact that Parisi establishes a virial expansion for lattice sphere packings, there is much sense in describing a fluid phase as the range of validity of this expansion. Moreover, as Parisi shows, for some purposes as  $d \rightarrow \infty$  the distribution of lattice points is well-approximated by an uncorrelated distribution of random points (see Section 4.4 of Ref.[15]). The so-called solid phase is associated with the densest lattice packing in a given dimension, the ground state of the system.

It is important to note here that while we can describe each configuration as a periodic pattern occupying the entire  $d$ -dimensional Euclidean space, this pattern is always composed of many copies of a single unit cell. Therefore, the system should be considered a spatially nonextended system in the sense that all its degrees of freedom are restricted to a single unit cell and once this unit cell is defined the entire periodic pattern in  $\mathbb{R}^d$  is prescribed. For any fixed value of  $d$ , the number of parameters required to fully describe the configuration of the system is finite, despite the fact that the positions of an infinite number of spheres are thus de-

scribed. Therefore, at any fixed  $d$ , the system does not have a thermodynamic limit, and any phase transition is in fact rounded. The role of the thermodynamic limit is filled by  $d \rightarrow \infty$ . This situation bares a resemblance to mean-field spin glass models where every pair (or p-tuple, as the case may be) of spins interact, such as the Sherrington-Kirkpatrick spin glass or the spherical p-spin glass [26].

As with classical hard spheres, the fluid phase remains metastable at densities above the crystallization point, and if the system is compressed quickly enough, it will reach a mechanically stable, jammed, structure without falling into the solid phase. In fact, in high dimensions, even very slow compression will lead to this result. According to the Random-First Order Transition (RFOT) theory, the system does experience a fluid-solid transition, but this solid phase is associated with one of many local maxima of the density, and not the global maximum [27]. At a finite pressure, the system will occupy many configurations in the basin of attraction around the local maximum, but as the pressure approaches infinity, the system configuration will approach the local maximum itself. Lattices that are local maxima of density in the space of valid packings are known in the literature as extreme lattices, and it is known that the number of contacts around any sphere in an extreme lattice cannot be smaller than  $z = d(d+1)$  [28]. This fact is similar, and indeed has similar origins, to the *isostatic* condition in the classical setting, which requires at least  $z = 2d$  contacts on average around each sphere. Classical jammed sphere packings are observed to also have no more than this number of contacts [29]. In Ref.[22], the authors identify tens of thousands of extreme lattices in dimensions  $d \leq 19$  as the final states of their algorithm. They find that an overwhelming majority in dimensions  $d \geq 17$  have exactly  $d(d+1)$  contacts. We call such lattices *isostatic*, and this notion of isostaticity should be contrasted with the classical notion of isostaticity, where an average of  $2d$  contacts are incident on each sphere.

The lattice sphere packing problem can be formulated as the following optimization problem over symmetric  $d \times d$  matrices:

$$\begin{aligned} & \text{minimize } \det G, \\ & \text{subject to } \langle \mathbf{n}, G\mathbf{n} \rangle \geq 1 \text{ for all } \mathbf{n} \in \mathbb{Z}^d \setminus \{0\}. \end{aligned} \quad (1)$$

Note that any feasible matrix  $G$  must be positive definite (depending on context, we will use the equivalent terms *feasible* which comes from the optimization literature and *admissible* from the geometry literature). A feasible matrix  $G$  corresponds to a packing of unit-diameter spheres, centered at the lattice points  $M\mathbf{n}$ ,  $\mathbf{n} \in \mathbb{Z}^d$ , where  $M$  is some matrix such that  $G = M^T M$  ( $M$  is determined by  $G$  only up to rotation). The choice of unit diameters fixes our scale for distances and wavenumbers, which will take dimensionless values in units of the sphere diameter and its inverse respectively. We call  $G$  the *Gram matrix* of the lattice, and  $M$  the *generating matrix*. The fraction of space filled by the packing is

$\varphi = 2^{-d}(\det G)^{-1/2}V_d$ , where  $V_d = \pi^{d/2}/\Gamma(\frac{d}{2} + 1)$  is the volume of a unit-*radius* ball in  $d$  dimensions. Note that the constraints in (1) actually come in equivalent pairs, since  $\langle \mathbf{n}, G\mathbf{n} \rangle = \langle -\mathbf{n}, G(-\mathbf{n}) \rangle$ .

Each *active* constraint (a constraint satisfied with equality), labeled by  $\mathbf{n}$ , corresponds to one contact per unit cell of the packing: namely between the sphere centered at  $M\mathbf{n}'$  and that at  $M(\mathbf{n}' + \mathbf{n})$  for any  $\mathbf{n}' \in \mathbb{Z}^d$ . We associate a contact force to this contact using the Lagrangian formulation of (1). A stationary point of the Lagrangian satisfies

$$(\det G)G^{-1} = \sum_{i=1}^z f_i \mathbf{n}_i \mathbf{n}_i^T, \quad (2)$$

where the sum runs over all contacts  $\mathbf{n}_i$ ,  $i = 1, \dots, z$ , and we assume that  $f_i = f_{i'}$  when  $\mathbf{n}_i = -\mathbf{n}_{i'}$  due to Newton's third law. Note that in contrast with the classical setting, this is not the same as simple mechanical force balance, since here we have force balance automatically from the equality of forces along contacts at antipodal points on the surface of the sphere. For stability, the forces must be repulsive  $f_i > 0$ . The criterion (2) with  $f_i > 0$  is known in the literature as *eutaxy* [28]. It turns out that an additional criterion for stability is that the rank-1 matrices  $\mathbf{n}_i \mathbf{n}_i^T$  have to form a complete basis of the space of symmetric  $d \times d$  matrices, a criterion known as *perfection* [28]. An equivalent definition of perfection is that the Gram matrix is fully determined by the identity of the contacts  $\mathbf{n}_i$ , that is, there is a unique Gram matrix such that  $\langle \mathbf{n}_i, G\mathbf{n}_i \rangle = 1$  for all  $i = 1, \dots, z$ . An admissible lattice which satisfies these two mechanical stability criteria is an extreme lattice, a local minimum of the optimization problem (1). The minimum number of contacts which makes this possible is the isostatic number  $z = d(d+1)$ . We limit our attention from this point on to isostatic extreme lattices. The average contact force can be obtained from (2) by multiplying both sides by  $G$  and taking the trace. Using the fact that  $\text{tr } \mathbf{n}_i \mathbf{n}_i^T G = \langle \mathbf{n}_i, G\mathbf{n}_i \rangle = 1$ , we have that  $\sum f_i = d(\det G)$  and so  $\langle f \rangle = (\det G)/(d+1)$ .

We will be interested in the distribution of distances between pairs of spheres in the lattice. Consider the function

$$Z(r) = |\{\mathbf{n} \in \mathbb{Z}^d : \langle \mathbf{n}, G\mathbf{n} \rangle \leq r^2\}| - 1,$$

which gives the number of spheres whose center is a distance of  $r$  or less from the center of some fixed sphere, not counting that sphere. This function is related to the more common pair correlation function  $g(r) = (dZ/dr)/(d^2 r^{d-1} \varphi)$ . The problem of finding the number of vectors in a lattice shorter than some length, given its generating matrix  $M$  or its Gram matrix  $G$ , is well studied and is known to be NP-hard [30].

The structure factor of the packing  $S(\mathbf{k})$  is given simply by the reciprocal lattice  $M^{-1}\mathbb{Z}^d$ :

$$S(\mathbf{k}) = \det M^{-1} \sum_{\mathbf{m} \in \mathbb{Z}^d} \delta(\mathbf{k} - M^{-1}\mathbf{m}).$$

Each nonzero point  $\mathbf{k}$  of the reciprocal lattice, if it is “visible” from the origin, corresponds to a partition of the direct lattice points into planes separated by a distance  $1/|\mathbf{k}|$ . Note that extremity imposes a constraint on the length of the shortest reciprocal lattice vector: a sphere in a given plane  $\langle \mathbf{k}, \mathbf{x} \rangle = 0$  must be in contact with at least  $d$  spheres in the half-space  $\langle \mathbf{k}, \mathbf{x} \rangle < 0$ , or else the planes defined by  $\mathbf{k}$  can be brought closer together and the lattice is not locally optimal in density. The largest possible separation along the direction of  $\mathbf{k}$  between the original sphere and the closest of the touching spheres is obtained when the spheres form a regular simplex, and the separation between the layers is  $\sqrt{(1 + \frac{1}{d})}/2$ . Therefore  $|\mathbf{k}| \geq \sqrt{2d/(d+1)}$  for any nonzero reciprocal lattice vector  $\mathbf{k}$ . This bound is achieved uniquely by the shortest reciprocal lattice vectors for the direct lattice generated by the root system  $A_d$ , which is in fact extreme and isostatic [1].

### III. METHODS

In Ref.[22] 10,000 lattice packings were generated in each dimension  $d = 10, \dots, 18$  and 100,000 in  $d = 19, 20$ . Using the same procedure, we generate 10,000 additional lattices in each dimension  $d = 21, \dots, 24$ , and in dimensions  $d = 19, 20$  we use only 20,000 of the 100,000 generated in Ref.[22]. The method used seeks to optimize the density using a sequence of moves, leading in some cases to the globally optimal solution and in other cases to a local optimum. Therefore, we expect the lattices obtained to be locally optimal, that is, extreme, but perhaps affected by numerical errors. For each lattice we calculate  $Z(1 + 5 \times 10^{-8})$ , the number of approximate contacts, and keep a record of the corresponding integer vectors  $\mathbf{n}$ . We keep all the lattices for which this number is exactly  $d(d+1)$ . Next, we reconstruct the Gram matrix from the identity of the contacts, which is guaranteed to be possible by perfection. However, due to numerical errors, for a small number of lattices the rank-1 matrices do not form a complete basis, and the reconstruction fails. We reject these lattices. Note that since we are using the integer vectors to determine the Gram matrix, we can achieve arbitrary precision, but for the purposes of this article, the precision of double precision floating point numbers suffices. We recalculate the number of neighbors using the precise Gram matrix, rejecting the small number of lattices that are not, after all, isostatic. Finally we calculate the contact forces by solving (2). Again, due to numerical errors in the original data we have to reject a small number of lattices that yield negative forces. The number of extreme isostatic lattices we end up with is given in Table I. For  $d \leq 14$ , only a small fraction of lattices generated are isostatic, but this fraction quickly grows to dominate the ensemble in higher dimensions. We suspect that this fraction should theoretically tend to one, but does not in our case because of numerical

| $d$ | Runs   | Extreme Isostatic |
|-----|--------|-------------------|
| 13  | 10,000 | 365               |
| 14  | 10,000 | 1,625             |
| 15  | 10,000 | 5,196             |
| 16  | 10,000 | 6,761             |
| 17  | 10,000 | 9,235             |
| 18  | 10,000 | 9,590             |
| 19  | 20,000 | 19,200            |
| 20  | 20,000 | 19,085            |
| 21  | 10,000 | 9,473             |
| 22  | 10,000 | 9,406             |
| 23  | 10,000 | 9,281             |
| 24  | 10,000 | 9,205             |

TABLE I: Number of runs of the algorithm of [22] used in each dimension  $d$ , and the number of extreme isostatic lattice obtained as a result of processing the resulting lattices according to the procedure outlined in Section III.

errors that make it difficult to exactly identify contacts. In Section IV we study the isostatic extreme lattices only in the dimensions where they constitute the majority of lattices generated, namely  $d \geq 15$ .

Our method of obtaining an ensemble of extreme lattices should be compared, perhaps, to the method used in Ref.[31]. There, the authors generate a large number of extreme lattices (tens of thousands) in dimensions  $d \leq 13$ . However, in higher dimensions, their method becomes inefficient and a much smaller number of distinct extreme lattices is generated (a few hundreds to a few thousands) in dimensions  $14 \leq d \leq 19$ . A major issue in Ref. [31] is that the method samples the same lattice multiple times, and therefore a large sample may contain only a small number of distinct lattices. With our methods we have no such issue: we find that any two lattices among our sample of extreme isostatic lattices in each dimension  $15 \leq d \leq 24$  have distinct values of the determinant, which implies necessarily that they are distinct. The two methods appear to complement each other well: the method of Ref.[31] is well-suited to generate large samples of distinct extreme lattices in dimensions  $d \leq 13$ , where the present method would produce many repetitions of the densest lattices, while the present method is well-suited for dimensions  $d \geq 14$ , where it produces hardly any repetitions among the isostatic extreme lattices.

## IV. RESULTS

### A. Densities

Understanding the distribution of densities at which hard spheres jam and its dependence on dimension is one of the major challenges facing the field. While it is now widely accepted that hard spheres can jam at a range of different densities [27, 32–34], different causes have been proposed to explain this variability: for example, vari-



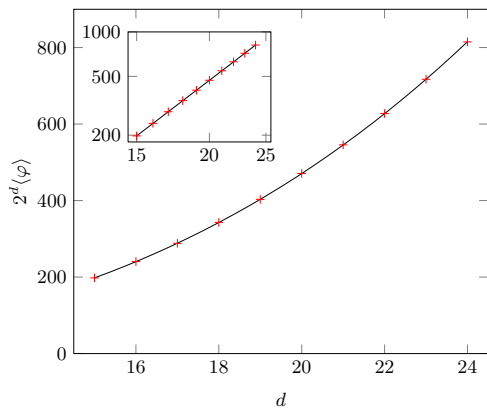


FIG. 1: The mean density  $\langle\varphi\rangle$  of jammed isostatic lattice sphere packings as a function of dimension, rescaled by  $2^d$ . The line is the best fit power law  $2^d\langle\varphi\rangle = 0.0567d^{3.01}$  and the inset shows the same on a log-log scale.

ability in the thermodynamic parameters of the initial configurations [35], or the existence of crystalline regions, detectable using a carefully constructed order parameter [36]. For a finite system, we always expect to observe a distribution of jamming densities. As the size of the system grows and if we use a fixed algorithm or experimental protocol to generate the packing, the distribution is expected to narrow and tend to a delta function as the thermodynamic limit is approached [37]. In general, the limit density depends on the algorithm used.

Additionally, different theories predict different scalings for the typical jamming density as a function of dimension. A local geometric argument based on a simple assumption for the pair correlation predicts  $\varphi \sim d2^{-d}$  [24]. A replica theory (RT) calculation also predicts a density  $\varphi_{\text{th}} \sim d2^{-d}$  [27], while a mode-coupling-theory (MCT) calculation predicts a MCT transition at a density  $\varphi_{\text{MCT}} \sim d^22^{-d}$ , implying that jamming must occur at an even higher density [7, 9, 10]. While our present results do not address any of these controversies directly, being obtained for a different system, we hope that they will nevertheless be useful in resolving them by providing both intuition and a convenient testing ground for theories.

The mean lattice density  $\langle\varphi\rangle$  as function of dimension is plotted in Figure 1. The dependence on the dimension is well-fit by  $\langle\varphi\rangle \simeq cd^\nu 2^{-d}$ , with  $\nu = 3.01 \pm 0.01$ . These densities are much higher than the jamming densities for classical hard spheres, and the relative difference is expected to widen with dimension. This result seems to be in stark contrast to the situation expected for the densest, rather than jammed, packings: in high enough dimensions, the densest packing of equal sized hard spheres is expected to be much denser than the densest (Bravais) lattice packing [5]. If the RT and MCT calculations can be carried over to the lattice setting, it would be interesting to see if any of them are contradicted by these results. The geometric calculation of Ref.[24] predicts a scaling

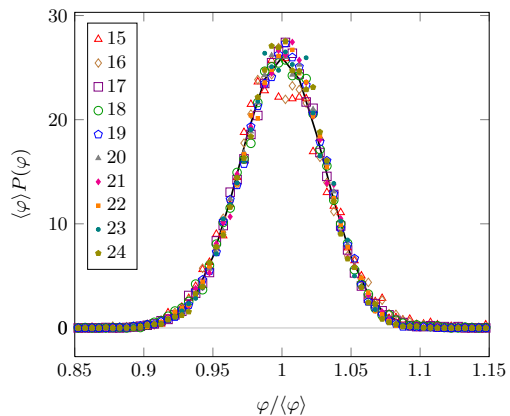


FIG. 2: The distribution of densities, rescaled by the mean density. The line is the best overall Gaussian fit.

$\varphi \sim z2^{-d}$ , which in this case would imply  $\varphi \sim d^22^{-d}$ .

In Figure 2 we plot the distribution of densities in each dimension rescaled by the mean density in that dimension. The distributions appear nearly identical, seemingly contradicting the expectation that the distribution should narrow as the system size grows. However, we note that the standard deviation of the distribution does show a slow narrowing trend: from  $3.3 \times 10^{-2}$  for  $d = 15$  to  $2.9 \times 10^{-2}$  for  $d = 24$ . We cannot predict from the current data whether the distribution will tend toward a delta function in the limit  $d \rightarrow \infty$ . We also note that the algorithm used here for different dimensions could arguably be considered not fixed, since it is not clear what the correct way to scale with dimension such parameters as the step size and the influence radius (see Ref. [22]). However, the persistence of a finite range of relative jamming densities in the thermodynamic limit even for a fixed algorithm might be possible due to the fact that the model has no spatial extent and is therefore not required to be self-averaging [26].

## B. Pair correlation

The pair correlation function  $g(r)$ , averaged over the jammed isostatic lattices in each dimension, is plotted in Figure 3. The pair correlation is zero for  $r < 1$  due to the hard-sphere constraint and has a delta-function singularity at  $r = 1$  due to the pairs that are in contact. For  $r > 1$  we observe a number of distinctive features: a power-law divergence  $g(r) \sim r^{-\gamma}$  for  $r \rightarrow 1^+$ , and apparent singularities at  $r = \sqrt{2}$  and  $r = \sqrt{3}$ . At finite-pressure the delta-function singularity at  $r = 1$  is also expected to broaden into a power-law, whose exponent is related to the distribution of contact forces and which will control the behavior at  $r \rightarrow 1^+$  [14, 38]. Since we are working with configurations at infinite pressure, the two singular behaviors at  $r = 1$  are completely separated, and can be studied separately in the pair-correlation  $g(r)$  and in the

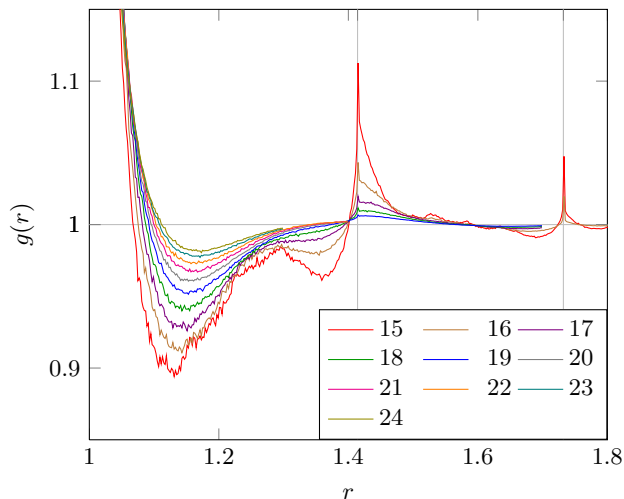


FIG. 3: The average pair correlation  $g(r)$  in a jammed isotropic lattice of dimension  $d$ , where  $d = 15, \dots, 24$ . The vertical lines mark the apparent singularities at  $r = \sqrt{2}$  and  $r = \sqrt{3}$ . The distances are given in units of the sphere diameter.

contact force distribution (see Section IV.C). Note that we were able to easily approach the infinite pressure limit in this system because a simple linear equation gives the exact Gram matrix once the contacts are identified. In the classical setting, the equations determining the configuration based on the identity of contacts are nonlinear, and highly nontrivial to solve. This is another remarkable advantage of the lattice model.

We observe that the features of  $g(r)$ , especially the singularities at  $r = \sqrt{2}$  and  $r = \sqrt{3}$ , become less pronounced in higher dimensions, and the correlation function approaches the asymptotic value  $g(\infty) = 1$  faster. The weakening of correlation features with increased dimension is a prediction of the principle of decorrelation [5]. This principle has been shown to apply not only to amorphous configurations but also to lattices [16].

While, for any individual lattice,  $g(r)$  is, strictly speaking, a sum of delta functions, the spacing between these is much smaller than the sphere radius, and  $g(r)$  can be considered a continuous curve (apart from the aforementioned singularities). Therefore, the curves in Figure 3, which are averaged over many lattices, can also be considered to represent the typical lattice. Note that this is a non-trivial feature of this ensemble of lattices. The extreme lattices that are densest, or close to densest, in any dimension are typically given by Gram matrices whose elements are rational numbers of small denominator [1, 22, 23]. Therefore, the possible squared pair separations  $r_{ij}^2 = \langle \mathbf{n}_i - \mathbf{n}_j, G(\mathbf{n}_i - \mathbf{n}_j) \rangle$  must also be rational numbers of small denominator, and the pair correlation function will consist, at least for  $r \lesssim 2$ , of only a few delta functions.

The divergence for  $r \rightarrow 1^+$  remains a strong feature for all the dimensions studied here. Such a divergence,

| $d$ | $\gamma$ | $\theta$ |
|-----|----------|----------|
| 15  | 0.3128   | 0.3534   |
| 16  | 0.3137   | 0.3685   |
| 17  | 0.3203   | 0.3633   |
| 18  | 0.3177   | 0.3603   |
| 19  | 0.3172   | 0.3654   |
| 20  | 0.3159   | 0.3731   |
| 21  | 0.3134   | 0.3834   |
| 22  | 0.3083   | 0.3856   |
| 23  | 0.3097   | 0.3830   |
| 24  | 0.3071   | 0.3775   |

TABLE II: The value in each dimension of the best-fit power law exponents for the data shown in Figure 4 and Figure 7.

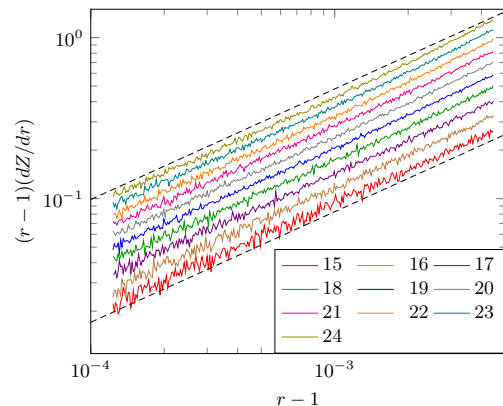


FIG. 4: Logarithmically binned histogram of pair separations. The curves are fit by power laws  $c(r-1)^{1-\gamma}$  with exponents given in Table II. The dashed lines have a slope of 0.686, corresponding to the average value of  $1-\gamma$ .

described by a power law, is also observed in classical jammed packings [38, 39], and the power law exponent seems to be independent of dimension [14]. We use logarithmic binning to extract the correlation of near-contacting pairs, which appears to be well-described by a power law  $\langle Z(1+\xi) \rangle \simeq A\xi^{1-\gamma}$  (see Figure 4). The best-fit values of  $\gamma$  are given in Table II. The value of the power law exponent seems to take a dimension-independent value of  $\gamma = 0.314 \pm 0.004$ . The amplitude of the near-contact singularity, on the other hand, seems neither to be a constant with dimension nor to be directly proportional to the density. Instead, the amplitude seems to scale with a distinct power law exponent as a function of dimension,  $A \simeq cd^{\tilde{\nu}}$ , where  $\tilde{\nu} = 3.30 \pm 0.05$  (see Figure 5).

### C. Forces

The distribution of the contact force at a random contact in a lattice, rescaled by the mean value for that lattice, is plotted in Figure 6. The mean value for each lattice is determined by its density (see Section II). Again we note that for any individual lattice, this distribution is discrete, but that it approaches a smooth distribution

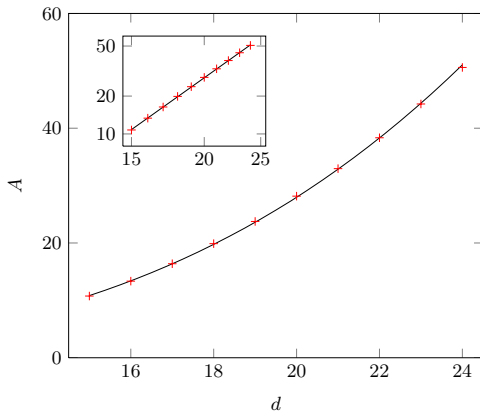


FIG. 5: The amplitude of the near-contact singularity in the pair correlation as a function of dimensions. The line is the best fit power law  $A = (1.43 \times 10^{-3})d^{3.30}$ . The inset shows the same on a log-log scale.

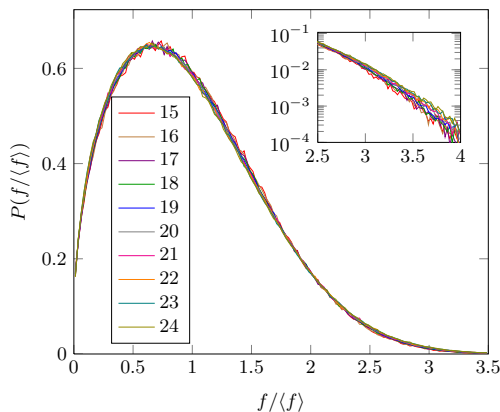


FIG. 6: The distribution of contact forces. The behavior of the tail of the distribution is shown in the inset on a semi-log plot.

as the number of contacts increases with dimension. For the densest lattices in any dimension, this is again not the case: not only are the contact forces not well-defined (because of hyperstaticity), but the high degree of symmetry implies that there are only a few inequivalent classes of contacts [1, 31].

Note that the distribution seems, already at the lowest dimensions studied here, to approach a limit distribution. The probability density peaks around the mean value and clearly goes to zero at zero force. Logarithmic binning of the forces reveals a power law dependence at low force of the form  $P(f/\langle f \rangle) = c(f/\langle f \rangle)^\theta$  (see Figure 7). Again, this behavior is consistent with the behavior of classical jammed packings [14]. The best-fit values of  $\theta$  are given in Table II and show that the power law exponent does not seem to depend on dimension and takes a value of  $\theta = 0.371 \pm 0.010$ .

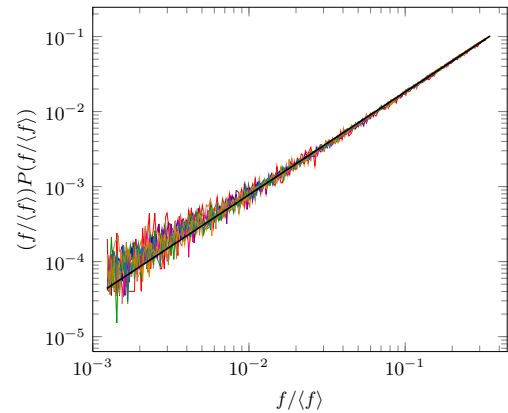


FIG. 7: Logarithmically binned histogram of contact forces. The black line shows the best fit power law  $(f/\langle f \rangle)P(f/\langle f \rangle) = 0.430(f/\langle f \rangle)^{1.371}$ .

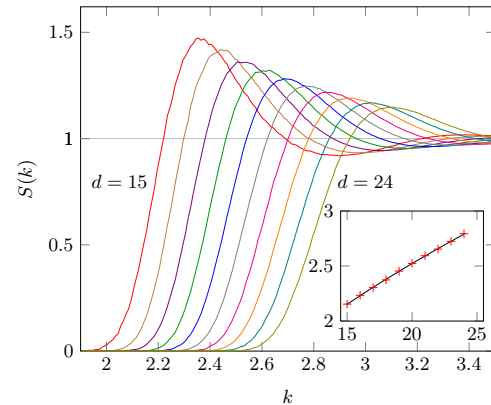


FIG. 8: Spherically averaged structure factor, averaged over all jammed isostatic lattices in each dimension. The inset shows the value of  $k$  such that  $S(k) = 1/2$  as a function of dimension. The wavenumbers are given in units of the inverse sphere diameter.

#### D. Structure factor

We plot the spherically averaged structure factor  $S(k)$ , averaged over all lattices in a given dimension, in Figure 8. As argued in Section II, the structure factor of an extreme lattice must vanish for a finite range of wave-numbers near  $k = 0$ , a property known as *stealth* [40]. Classical jammed packings, by contrast, tend to have a structure factor which approaches 0 continuously at  $k = 0$  [41]. While the stealth wavenumber for an extreme lattice must be greater than  $\sqrt{2d/(d+1)}$  (its value for the wholly atypical lattice  $A_d$ ), its value for the typical jammed lattice seems to be significantly larger, and to increase with dimension (see inset of Figure 8). The amplitude of the oscillations about the value  $S(k) = 1$  for large  $k$  become smaller and smaller with dimension, as expected by the decorrelation principle [5, 16].

Apart from the low-wavenumber behavior, these structure factors bare a marked resemblance to those observed

in classical jammed packing [6, 42, 43]. Those structure factor do not exhibit stealth, but are instead heavily suppressed at small wavenumbers, followed by a sharp rise and then oscillations about  $S(k) = 1$  that decay as  $k \rightarrow \infty$ . The height of the first peak in  $S(k)$  decreases with increasing dimension and the wavenumber at which it appears increases.

## V. CONCLUSION

Due in part to similarities observed between the phenomenology of structural glasses and of the spherical p-spin glass model, there has been an effort over the last decade to understand the glass transition and jamming in hard-sphere systems by studying models with no spatial extent [27]. In most cases, the network of interactions between different degrees of freedom in these models are sparse graphs or trees [44–46]. However, the interactions in the spherical p-spin model are dense: every p-tuple of spins interacts. Also, while it appears that much progress can be made in understanding some general behavior using these models, much is lost in the process about the distinct structural features of jamming. Features such as the power law behaviors of weak contacts and small

gaps play a major role in determining the stability of jammed states [47, 48], yet so far they have been missed completely in replica theory calculations [14]. In this article, we presented a spatially nonextended model of hard spheres with a dense interaction network that retains nearly all of the structural features of the classical hard-sphere model. We have examined some of the phenomena exhibited by jammed isostatic lattices, as manifested in their densities, pair correlations, contact force distributions, and structure factors, and the relation to similar phenomena exhibited in the classical hard-sphere model. The lattice hard-sphere model enables numerical exploration of these phenomena in much higher dimensions than was previously possible. We have only begun exploring this rich set of phenomena, and there is clearly much work still to be done.

**Acknowledgements.** S. T. and É. M. were supported in part by the Materials Research Science and Engineering Center Program of the National Science Foundation under Grant No. DMR-0820341 and by the Division of Mathematical Sciences at the National Science Foundation under Award No. DMS-1211087. This work was partially supported by a grant from the Simons Foundation (Grant No. 231015 to Salvatore Torquato).

- 
- [1] J. H. Conway and N. J. A. Sloane, *Sphere Packings, Lattices, and Groups (Third Edition)* (Springer, New York, 1998).
  - [2] H. Minkowski, *J Reine Angew Math* **1905**, 220 (1905).
  - [3] K. Ball, *Int Math Res Notices* **1992**, 217 (1992).
  - [4] S. Torquato, O. U. Uche, and F. H. Stillinger, *Phys Rev E* **74**, 061308 (2006).
  - [5] S. Torquato and F. H. Stillinger, *Exper Math* **15**, 307 (2006).
  - [6] M. Skoge, A. Donev, F. H. Stillinger, and S. Torquato, *Phys Rev E* **74**, 041127 (2006).
  - [7] P. Charbonneau, A. Ikeda, G. Parisi, and F. Zamponi, *Phys Rev Lett* **107**, 185702 (2011).
  - [8] J. A. van Meel, B. Charbonneau, A. Fortini, and P. Charbonneau, *Phys Rev E* **80**, 061110 (2009).
  - [9] B. Schmid and R. Schilling, *Phys Rev E* **81**, 041502 (2010).
  - [10] A. Ikeda and K. Miyazaki, *Phys Rev Lett* **104**, 255704 (2010).
  - [11] P. Charbonneau, A. Ikeda, G. Parisi, and F. Zamponi, *Proc Nat Acad Sci USA* **109**, 13939 (2012).
  - [12] J. Kurchan, G. Parisi, and F. Zamponi, *J Stat Mech* **2012**, P10012 (2012).
  - [13] S. Torquato and Y. Jiao, *Phys Rev E* **82**, 061302 (2010).
  - [14] P. Charbonneau, E. I. Corwin, G. Parisi, and F. Zamponi, *Phys Rev Lett* **109**, 205501 (2012).
  - [15] G. Parisi, *J Stat Phys* **132**, 207 (2008).
  - [16] C. E. Zachary and S. Torquato, *J Stat Mech* **2011**, P10017 (2011).
  - [17] L. V. Woodcock, *J Chem Soc, Faraday Trans 2* **72**, 731 (1976).
  - [18] R. L. Davidchack and B. B. Laird, *Phys Rev Lett* **85**, 4751 (2000).
  - [19] L. V. Woodcock, *J Chem Soc, Faraday Trans 2* **72**, 1667 (1976).
  - [20] H. M. Jaeger and S. R. Nagel, *Science* **255**, 1523 (1992).
  - [21] M. Engel, J. A. Anderson, S. C. Glotzer, M. Isobe, E. P. Bernard, and W. Krauth, *Phys Rev E* **87**, 042134 (2013).
  - [22] É. Marcotte and S. Torquato, *Phys Rev E* **87**, 063303 (2013).
  - [23] Y. Kallus, *Phys Rev E* **87**, 063307 (2013).
  - [24] Y. Jin, P. Charbonneau, S. Meyer, C. Song, and F. Zamponi, *Phys Rev E* **82**, 051126 (2010).
  - [25] T. M. Thompson, *From Error Correcting Codes Through Sphere Packings to Simple Groups* (Math Assoc Amer, Washington, 1984).
  - [26] T. Castellani and A. Cavagna, *J Stat Mech* **2005**, P05012 (2005).
  - [27] G. Parisi and F. Zamponi, *Rev Mod Phys* **82**, 789 (2010).
  - [28] J. Martinet, *Perfect Lattices in Euclidean Spaces* (Springer, Berlin, 2003).
  - [29] A. Donev, R. Connelly, F. H. Stillinger, and S. Torquato, *Phys Rev E* **75**, 051304 (2007).
  - [30] D. Micciancio, *SIAM J Compu* **30**, 2008 (2001).
  - [31] A. Andreanov, A. Scardicchio, and S. Torquato (2013), arXiv:1309.1301.
  - [32] S. Torquato and F. H. Stillinger, *Rev Mod Phys* **82**, 2633 (2010).
  - [33] P. Chaudhuri, L. Berthier, and S. Sastry, *Phys Rev Lett* **104**, 165701 (2010).
  - [34] Y. Jiao, F. H. Stillinger, and S. Torquato, *J Appl Phys* **109**, 013508 (2011).
  - [35] A. J. Liu, S. R. Nagel, W. van Saarloos, and M. Wyart, in *Dynamical heterogeneities in glasses, colloids, and gran-*



- ular media*, edited by L. Berthier, G. Biroli, J. Bouchaud, L. Cipeletti, and W. van Saarloos (Oxford University Press, 2010).
- [36] S. Torquato, T. M. Truskett, and P. G. Debenedetti, *Phys Rev Lett* **84**, 2064 (2000).
  - [37] C. S. O'Hern, L. E. Silbert, A. J. Liu, and S. R. Nagel, *Phys Rev E* **68**, 011306 (2003).
  - [38] A. Donev, S. Torquato, and F. H. Stillinger, *Phys Rev E* **71**, 011105 (2005).
  - [39] L. E. Silbert, A. J. Liu, and S. R. Nagel, *Phys Rev E* **73**, 041304 (2006).
  - [40] R. D. Batten, F. H. Stillinger, and S. Torquato, *J Appl Phys* **104**, 033504 (2008).
  - [41] A. Donev, F. H. Stillinger, and S. Torquato, *Phys Rev Lett* **95**, 090604 (2005).
  - [42] S. Torquato and F. H. Stillinger, *J Phys Chem B* **106**, 8354 (2002).
  - [43] B. Charbonneau, P. Charbonneau, Y. Jin, G. Parisi, and F. Zamponi, *J Chem Phys* **139**, 164502 (2013).
  - [44] O. Rivoire, G. Biroli, O. C. Martin, and M. Mézard, *Eur Phys J B* **37**, 55 (2004).
  - [45] F. Krzakala, M. Tarzia, and L. Zdeborová, *Phys Rev Lett* **101**, 165702 (2008).
  - [46] R. Mari, F. Krzakala, and J. Kurchan, *Phys Rev Lett* **103**, 025701 (2009).
  - [47] M. Wyart, *Phys Rev Lett* **109**, 125502 (2012).
  - [48] E. Lerner, G. Düring, and M. Wyart, *Soft Matter* **9**, 8252 (2013).